

# Scalar Potential Topography can Simplify Interpretation of 2D Vector Fields

Richard Chasen Spero\*

Department of Physics and Astronomy, University of North Carolina at Chapel Hill

Russell M. Taylor II†

Department of Computer Science, University of North Carolina at Chapel Hill

## Abstract—

We demonstrate a new visualization technique to help researchers answer specific questions about 2D vector fields. Rather than directly display the vector field, the visualization isolates the integrable part of the field, integrates it to find a scalar potential, and displays the scalar potential as a height field. Scalar potential representation can be combined with direct field representation, by overlaying a representation of either the original field or its divergence-free part. Representing a vector field by its scalar potential is useful for answering questions about bulk flow across a flow field, and for comparing vector fields. It leverages human intuition about how water flows downhill.

## 1 INTRODUCTION

Many visualization techniques exist for vector fields in two dimensions, and their relative utility has been thoroughly studied [7]. Interestingly, the inanimate techniques for vector field visualization share an important similarity: they all directly represent the vector field lines. Essentially, they emulate the effect of iron filings on paper in the presence of a magnet, conveying by their orientation and density the strength and direction of the field.

Naturally, these techniques are so prevalent precisely because scientists can use them to answer questions they ask when interpreting vector fields. Using the metaphor of flow along the surface of a fluid, some of the common questions are:

1. To where does a floating cork travel, given a starting position?
2. How fast does a floating cork move?
3. What are the sources and sinks of fluid?
4. Where are the saddle-points of fluid flow?

Direct representation of the vector field is less effective at conveying information about bulk characteristics of vector fields. For example, it can be difficult to answer the following questions using direct field representation:

1. What is the net fluid flow across a region of an image?
2. What is the relative output of sources in the field?
3. Are there similar features (sources, sinks, saddles) at different locations in two different vector fields?

In the present work, we demonstrate a new visualization technique designed to answer these questions. It is an alternative to direct field representation that isolates the integrable part of the field, integrates it to find a scalar potential, and displays the scalar potential as a height field.

\*e-mail: rspero@physics.unc.edu

†e-mail: taylorr@cs.unc.edu

- R.C. Spero is with the Department of Physics and Astronomy, University of North Carolina at Chapel Hill.
- R.M. Taylor is with the Department of Computer Science, University of North Carolina at Chapel Hill.

## 1.1 Prior Work

Vector field display techniques have a long history. Modern approaches fall under glyph- and texture-based techniques. These can be extended by mixing the two, using animation, or analyzing the field prior to display.

*Glyph-based methods* present characteristics of the flow at various locations. Straight or curved lines indicate local flow, and adding arrowheads disambiguates flow direction. Careful placement greatly improves the display [18].

*Texture-based methods* generate a dense display of flow information on surfaces. Spot noise parameterized by the flow field can produce patterns indicating flow [20]. Line-integral convolution (LIC) advects a noise texture along the flow direction, producing a dense display of flow direction [2]. Anisotropic nonlinear diffusion has been used to produce dense textures that indicate flow direction and magnitude [13]. Reaction-diffusion simulations can produce patterns that indicate flow direction and speed [14]. Gabor filters parameterized by the flow can indicate flow and flow magnitude [22].

*Mixed methods.* Sometimes these display techniques are used in combination, as when overlaying simplified arrow representations on top of LIC [16], or when using painterly layering techniques to display combined tensor, vector, and scalar fields in the same display [6]. Streamlines can be used at high density to produce LIC-like textures [21]. Coloring individual strands of texture-based methods enables the display of multiple scalar fields along with the vector data [19]. Animated LIC [9, 15, 23] disambiguates the flow direction.

*Analytic methods.* There is work on converting from vector representation to scalar fields for display, including pattern-matching to locate desired flow features [3]. There are techniques for decomposing flow fields into source/sink, vortex, and other portions [17].

Using this nomenclature, the scalar potential representation on which we report here is an analytic method that can be mixed with either glyph or texture-based methods.

## 2 VECTOR FIELD DECOMPOSITION AND INTEGRATION

Formally, a scalar potential exists for all curl-free vector fields. For an arbitrary field, the part with curl can be subtracted from the original field and the difference can be integrated to find a scalar potential. This requires decomposing the vector field.

An arbitrary vector field  $\mathbf{A}(x, y)$  can be expressed as the sum of three fields

$$\mathbf{A}(x, y) = \mathbf{v}(x, y) + \mathbf{w}(x, y) + \mathbf{z}(x, y), \quad (1)$$

such that

$$\nabla \times \mathbf{v} = 0 \quad \nabla \cdot \mathbf{w} = 0 \quad \mathbf{z} = \mathbf{A} - \mathbf{v} - \mathbf{w}.$$

where  $\nabla$  is the vector operator

$$\nabla = \frac{\partial}{\partial x} \hat{x} + \frac{\partial}{\partial y} \hat{y} + \frac{\partial}{\partial z} \hat{z},$$

$\hat{x}$ ,  $\hat{y}$ , and  $\hat{z}$  are the unit vectors along the  $x$ ,  $y$ , and  $z$  axes, and  $\nabla \cdot$  and  $\nabla \times$  are the vector operations divergence and curl.

The curl-free fields  $\mathbf{v}$  and  $\mathbf{z}$  are conservative, such that the field  $\mathbf{F} = \mathbf{v} + \mathbf{z}$  is integrable<sup>1</sup> (and the vector field  $\mathbf{w}$  is not):

$$\oint (\mathbf{v} + \mathbf{z}) dl = 0,$$

where  $l$  is any closed path integral inside the image. For conservative fields, there exists a single-valued scalar potential  $\Phi(x, y)$ , such that

$$-\nabla \Phi(x, y) = \mathbf{v}(x, y) + \mathbf{z}(x, y) = \mathbf{F}(x, y). \quad (2)$$

The scalar potential  $\Phi$  is unique up to a constant. The core approach of the technique presented here is to calculate  $\Phi$  and map it as a height field.

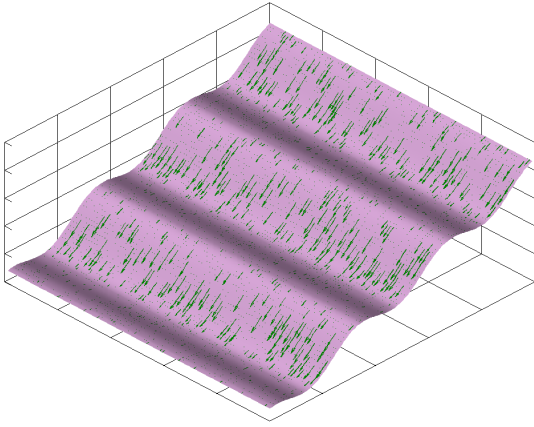


Fig. 1. The metaphorical scalar potential for the vector field  $\mathbf{A} = -\hat{x}(2 - 3 \sin \frac{\pi x}{10})$ . For reference,  $\mathbf{A}$  is projected onto the surface. Notice a droplet placed at any location on this surface will slide in the same direction as  $\mathbf{A}$ .

## 2.1 Metaphorical Scalar Potential for a 2D Force Field

Before describing how to calculate  $\Phi$ , we offer an explanation of why this visualization technique works. We intuitively interpret a common type of vector field—the force due to gravity—using its scalar potential. The scalar potential of a force field is the potential energy stored by an object as it is displaced through the field. Pushing a block up a hill stores gravitational potential energy in the block. We understand intuitively that there is a direct relationship between the potential energy in the block and how high it has gone up the hill. Specifically, gravitational potential energy is proportional to height:

$$U \propto h.$$

By looking at the topography of a surface, we can easily predict where a block would slide given a starting position.

Although we have good intuition for interpreting this simple system, it is a three dimensional problem and not obviously extensible to arbitrary 2D vector fields. Like many other visualization techniques, this one relies on a metaphor: where the original data encode, say, the velocity of a fluid over a 2D area, the visualization will invite the user to imagine a droplet sliding on a 2D surface in a 3D environment.

<sup>1</sup>Here we define *integrable* as the gradient of a unique scalar potential.

In detail, we construct a *metaphorical* scalar potential  $\Phi_m$  from a *metaphorical* surface gradient  $\mathbf{m}$ , given the integrable 2D vector field  $\mathbf{F}$  of Equation 2. We are looking to create  $\Phi_m$  such that motion due to gravity of a probe on its surface mimics the motion of a probe in  $\mathbf{F}$ . Because the metaphorical surface is in 3D and relies on our intuition about gravity, it is not obvious what the relationship between  $\mathbf{m}$  and  $\mathbf{F}$  should be. However, in the Appendix we demonstrate that the simplest possible relationship,  $\mathbf{m} = \mathbf{F}$ , is acceptable.

## 2.2 Implementation

In the present work, Matlab was used for all calculations and to generate all figures. For an arbitrary 2D vector field  $\mathbf{A}(x, y)$  we begin by calculating  $\mathbf{w}$ :

$$\mathbf{J}(x, y) = \nabla \times \mathbf{A}$$

$$\mathbf{w} = \int_S \frac{\mathbf{J}(x', y')}{|\mathbf{r} - \mathbf{r}'|^3} \times (\mathbf{r} - \mathbf{r}') dr',$$

where  $S$  is the area of the image and  $r$  and  $r'$  are the radial position vectors from the image origin to a point  $(x, y)$  and  $(x', y')$ , respectively. We used Matlab's `curl` and `trapz` functions for differentiation and integration. With  $\mathbf{w}$  in hand, we find the integrable field  $\mathbf{v} + \mathbf{z}$  from  $\mathbf{A} - \mathbf{w}$ , using Equation 1.

Using the result of Section 2.1, we can find  $\Phi_m$  by integrating  $\mathbf{F}$  over the area of the image. We use the technique of Frankot and Chellappa [5] because this method enforces integrability; we use it in the hope of suppressing any artifacts generated during the calculation of  $\mathbf{w}$ . Briefly, we calculate the Fourier transform of  $m_x$  and  $m_y$ , then integrate the field in the frequency domain. The resultant scalar field is transformed back to the spatial domain.

Discontinuity in  $\mathbf{F}$  can be problematic for this method of integration, but many vector fields are non-zero at the boundary. Therefore, to ensure proper behavior at the boundaries during integration, we pad the image by repeating its border, making the image approximately 6-8 times its original size, then scale the field by a 2 dimensional hamming window. After integration, we remove the padding. To ensure proper integration of any constant background field, we separate out the average value of the field, integrate it in the spatial domain, and add the resulting linear scalar field to  $\Phi_m$ .

This implementation is relatively straight-forward, but other approaches may be more appropriate for specific applications. We note that Polthier and Preuss have reported on vector field decomposition using both the variational technique and Hodge decomposition [11, 12]. For applications where all field sources reside outside the image (namely,  $\mathbf{A} = \mathbf{z}$ ), or generally whenever  $\mathbf{w} = 0$ , the vector field is already known to be integrable, so no decomposition of  $\mathbf{A}$  is required and it is sufficient to set  $\mathbf{F} = \mathbf{A}$ .

## 3 ANSWERING QUESTIONS

To use this visualization to interpret flow fields, the user must learn to interpret the height field of  $\Phi_m$ . Figure 1 shows a simple vector field in which  $\nabla \Phi_m = -\mathbf{F} = -\mathbf{A}$  (i.e.,  $\mathbf{w} = 0$ ). How can the user answer the question, “Where will a probe travel?”

Imagine a droplet of liquid, which moves when the slope is nonzero, but which stops as soon as it reaches a flat surface. A droplet of water starting at the top right of the image would slide into the first trough, then stay there permanently. Checking against the direct field representation, we see that indeed, each trough in  $\Phi_m$  is sink and each ridge is a source, running vertically along the image.

Why is the “sliding droplet” metaphor the correct interpretation? Intuitively, we imagine a probe on the surface  $\Phi_m$  being pulled by gravity. But the original vector field  $\mathbf{A}$  is a velocity field, so our imagined probe-surface interaction should be the kind where the probe velocity is proportional to the force applied by gravity. Such systems are called over-damped. In the sliding droplet metaphor, the friction between the droplet and the surface halts the low-mass droplet as soon as it reaches a local minimum.

We are now ready to analyze sample vector fields.

### 3.1 Basic Questions

Scalar potential topography can be used to interpret the field from which it was integrated. Following are common questions about vector fields, and the interpretation used in direct field and scalar potential representations.

1. Where does the flow go?

Direct field representation: the user imagines a floating cork being pushed along the field lines.

Scalar potential representation: the user imagines a sliding droplet.

2. How fast is the flow?

Direct Field Representation: the user examines glyph properties (e.g. size of arrow) or field line density.

Scalar potential representation: the user examines the slope of the height field.

3. Where are the sources and sinks?

Direct field representation: the user looks for divergence and convergence of field lines.

Scalar potential representation: the user looks for peaks and pits in the surface.

4. Where are the saddle points in the flow?

Direct field representation: the user looks for divergence along one axis and convergence along another.

Scalar potential representation: these points appear explicitly as saddles in the surface.

For curl-free vector fields, all of the information in  $\mathbf{A}$  is included in the scalar potential. But common simulations and experiments result in turbulent or otherwise non-integrable fields. With such fields, scalar potential topography can still be used to identify sources and sinks of flow, as these are due to the diverging field  $\mathbf{v}$ .

The scalar potential representation of the integrable part of  $\mathbf{A}$  can be misleading, particularly in areas where  $|\mathbf{w}| \geq |\mathbf{F}|$ . In these regions, the actual direction or magnitude of  $-\nabla\Phi$  may deviate wildly from  $\mathbf{A}$ . Overlaying a direct field representation of  $|\mathbf{A}|$ , as in Figures 1, 3, and 6, can mitigate confusion while permitting the interpretations discussed in the following sections.

Under certain circumstances, it may be illuminating to instead overlay  $\mathbf{w}$ , as in Figures 4 and 7.

### 3.2 New Questions

#### 3.2.1 Comparing Source Output

Because the scalar potential is the integral of a vector field, its advantages emerge when interpreting field behavior over large areas. As a simple example, consider the flow field in Figure 2 produced by two sources. A direct field representation leaves it unclear which source pumps in more fluid. However, the scalar potential represents the volume of fluid per time moving away from a given point in the image. Therefore, simply comparing the heights of the two peaks in the scalar potential representation reveals which source is greater.

#### 3.2.2 Bulk Flow and Field Comparison

Our collaborators, who are studying microfluidic fluid transport as detailed in Section 4, are among those who ask the question, “What is the bulk flow across a region of a vector field?” Bulk flow may take many forms, including net flow across the whole image, or divergence from a source inside the image, but it necessarily indicates some global motion of fluid over some region. Scalar potential proves to be a useful way to reveal whether and where there is bulk flow in an image.

Figure 3 presents two vector fields both directly and as scalar potentials. The direct field representations are complicated, and the bulk flows in the image are difficult to determine and describe. The scalar

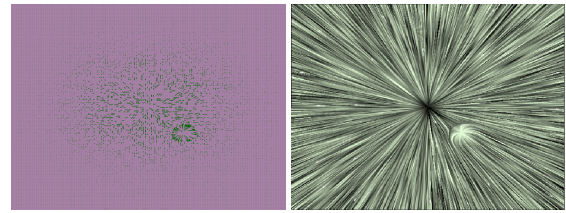


Fig. 2. The direct (top) and scalar potential (bottom) representations of a curl-free field ( $\mathbf{w} = 0$ ). Although the source in the bottom right is stronger at the center, its total output is lower.

potentials, however, clearly demonstrate that a droplet on either surface would slide in  $-\hat{y}$ . The sources are also easy to identify; these are the regularly spaced ridges and the peak present in both images.

We also note that the scalar potential representations are easy to compare across images. The scalar potentials reveal that there are two peaks that have similar shape and stand similar heights above the background field, indicating sources of similar output. Similarly, there is a sinusoidal topography in  $\hat{x}$  that is of similar frequency in both images, but varies in phase, indicating that there are vertical sources and sinks, regularly spaced, but offset in  $\hat{x}$ .

#### 3.2.3 Compatibility with Direct Representation

The height field representation of a vector field is conveniently compatible with existing glyph-based techniques, making it possible to overlay both in the same display. One possibility is to texture map a direct representation of the original field  $\mathbf{A}$ . In cases where  $\mathbf{w} = 0$ , as in Figure 1, overlaying a direct representation of the field itself can serve to redundantly encode information about the flow. In cases where  $\mathbf{w} \neq 0$ , as in Figure 3, it can provide context. For example, the overlay highlights that in certain parts of the image, the fluid sources are overwhelmed by the swirling field.

Alternatively, it is possible to overlay just the part of  $\mathbf{A}$  that is not represented by the scalar potential—namely,  $\mathbf{w}$ . In Figure 4 we project  $\mathbf{w}$  onto  $\Phi_m$ , so all of the data from  $\mathbf{A}$  is represented. Note that displaying  $\mathbf{w}$  separate from the rest of  $\mathbf{A}$  helps us compare the vortical parts of the two fields. Separated from the integrable parts of the field, the centers of these vortices can be located and their differences in radial dependence examined.

## 4 APPLICATION: MICROFLUIDIC FLOW AND MIXING

Our research group builds high-aspect ratio, superparamagnetic, polymer nano-rods that can be magnetically actuated [4]. Mechanisms for controlling flow and enabling mixing of microliter quantities of fluid are attracting increasing attention [8, 10]. We have found that scalar potential topography is a useful tool for interpreting the fluid flow generated in these environments.

We film fluorescent tracers in the liquid around the nanorods, then apply an optical flow computation to the movie using in-house soft-

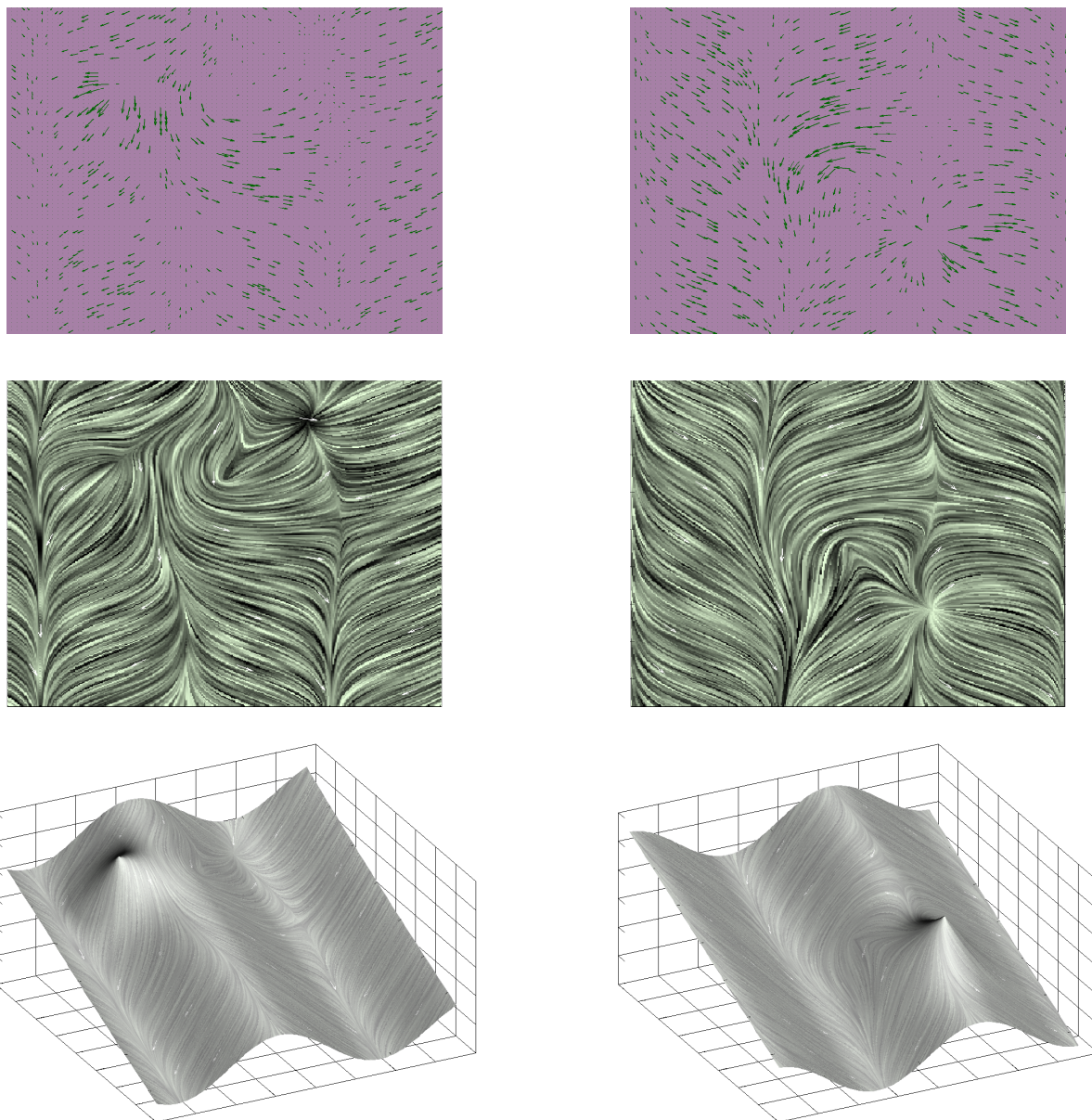


Fig. 3. Direct representation and scalar potentials for two vector fields. Note that it is difficult to interpret bulk flow or compare the fields using the quiver plots (top) or LIC (middle). The scalar potentials (bottom), rendered with a low-contrast LIC overlay of  $\mathbf{A}$ , reveal similarities and differences of the fields, including: (1) a source is hidden in the upper left corner of the field on the left, which is similar in output to the source in the lower right corner of the field on the right, (2) there is a similar bulk flow from the top to bottom of these images, and (3) periodic sources and sinks exist in both fields, but are shifted horizontally from one image to the other.

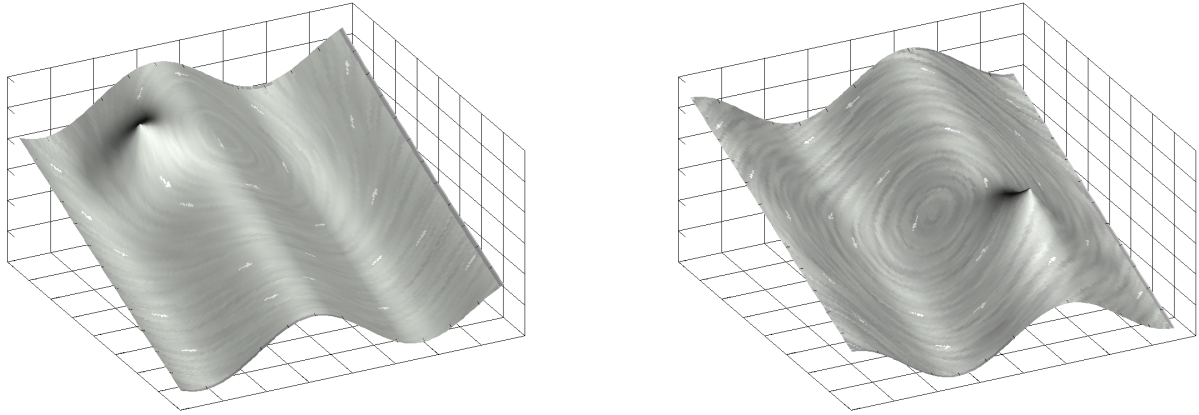


Fig. 4. Overlaying only  $\mathbf{w}$  on the scalar potentials from Figure 3 makes it possible to compare the position, size, and radial dependence of the curling part of the field.

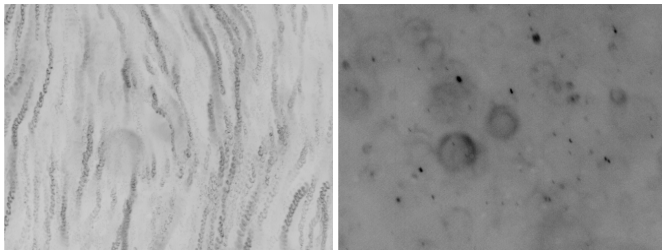


Fig. 5. (left) An inverted maximum intensity projection (similar to streamlines) of a video showing fluorescent tracer particles moving due to fluid flow generated by nanorod actuation. (right) A single contrast-enhanced frame highlights circular artifacts in the center of the image. These corrupt the optical flow computation and appear as artifacts in the scalar potential (Figure 6, bottom right). They are encircled by the curling part of the field, as seen in Figure 7.

ware, ImageTracker. The computation combines local texture information and a global smoothness constraint as in [1]. In the present work, ImageTracker outputs a 2D vector field of the fluid flow integrated over the length of the movie.

In Figure 6 we present two such fields, one of the integrated flow after four seconds, and one after 30 seconds. The movie is 30 fps. In this experiment we vary the integration window because the flow behavior may change as we increase the timescale.

The direct field representation presents some problems for interpreting these flow fields. At short timescales, it is difficult to interpret a quiver plot of the flow, due to a few large-magnitude glyphs that overwhelm the rest of the field. LIC is agnostic of field magnitude, and so clarifies the texture of the field at the expense of communicating the field strength. A long timescales, it is not clear how consistent the bulk flow of the field is.

We can interpret the flows more fully using the fields' scalar potential topographies. We can simultaneously interpret the large-magnitude and small-magnitude areas of the short timescale image. We can see that the wild fluctuations in magnitude disappear at long timescales, and we can resolve the constant background flow across the image.

There is a divot in the scalar potential of the long timescale video (Figure 6, bottom right) that highlights an error in the image flow computation. Tracer particles occasionally stick to the nanorods, producing circular artifacts (Figure 5, right). Interestingly, this region of corrupted flow computation is encircled by the dominant flow in  $\mathbf{w}$ , as

shown in Figure 7. Thus, we speculate that the non-integrable field may help identify artifacts in future video analysis.

## 5 CONCLUSIONS

We have implemented a new visualization technique, scalar potential representation of 2D vector fields, that helps users more easily answer specific questions about vector data. These questions include issues relating to field comparison and characterizing bulk flow in an image.

Additionally, we have demonstrated that scalar potential representation integrates well with existing techniques for direct field representation, and have used this combination to gain insight into a specific research problem.

## 6 APPENDIX: EQUATING METAPHORICAL AND MATHEMATICAL POTENTIALS

For an integrable 2D vector force field  $\mathbf{F}$ , we want to calculate a *metaphorical surface* on which a block would slide according to  $\mathbf{F}_{3D}$ , the net force on the block, such that the block's velocity would have the same speed and the same horizontal direction as a probe in the original field  $\mathbf{F}$ . We proceed by finding relationship between  $\mathbf{F}_{3D}$  and the gradient of the metaphorical surface.

Consider the force on a block of unit mass, sliding over a surface. The force varies with the surface gradient  $\mathbf{m}$ :

$$|\mathbf{F}_{3D}(x,y)| = g \sin(\theta(x,y)), \quad \sin(\theta(x,y)) = \frac{|\mathbf{m}(x,y)|}{\sqrt{1 + |\mathbf{m}(x,y)|^2}}, \quad (3)$$

where  $\theta$  is the angle the surface makes with the horizontal, and  $g$  is a constant implying the acceleration of the block due to metaphorical gravity. Note that  $\mathbf{F}_{3D}$  is a 3-dimensional vector with a 2-dimensional input. We can now solve Equations 3 for the magnitude of the surface gradient,

$$|\mathbf{m}| = |\mathbf{F}_{3D}| \sqrt{g^2 - |\mathbf{F}_{3D}|^2}$$

Our perception of the block's motion on the surface does not depend critically on the scaling of the surface, so we can divide  $\mathbf{m}$  by  $g$  with impunity. We can also obtain the direction of  $\mathbf{m}$  by noting that it always points in the direction of  $\mathbf{F}$ . Finally, we choose  $|\mathbf{F}_{3D}(x,y)| = |\mathbf{F}(x,y)|$ , so we may drop the 3D subscript from  $\mathbf{F}$ :

$$\mathbf{m} = \mathbf{F} \sqrt{1 - \frac{|\mathbf{F}|^2}{g^2}} \quad (4)$$

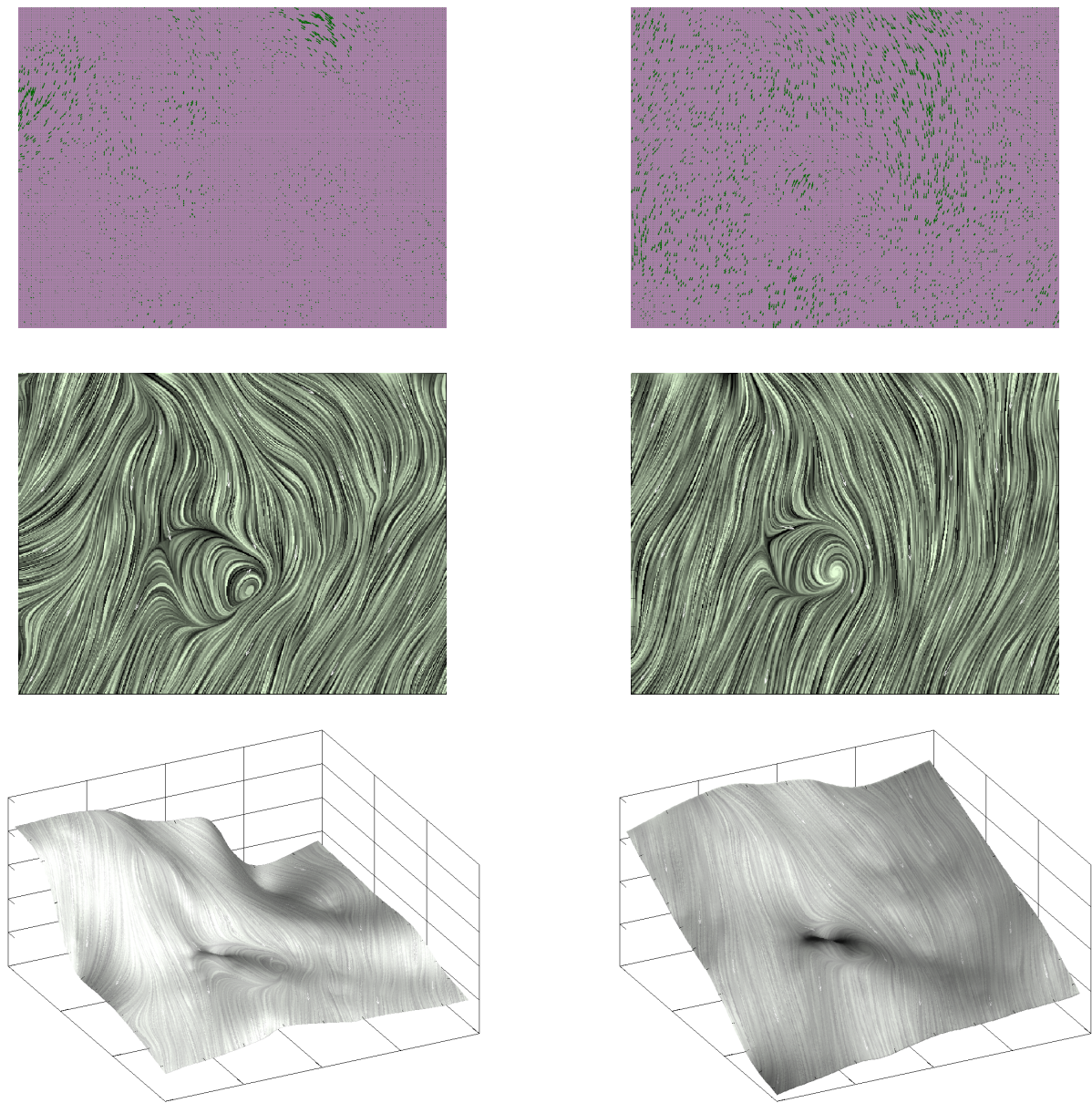


Fig. 6. Direct field representation of fluid flow at short (left) and long (right) timescales. Sharp variations in field magnitude make it difficult to interpret the field when the glyphs are scaled by field magnitude (top). Exchanging quiver plots for LIC (middle) clarifies the texture of the field at the expense of communicating the field strength. From scalar potential topography (bottom) we can interpret the field everywhere in the image and resolve the constant background flow. The flow direction is redundantly encoded by overlaying LIC of  $A$

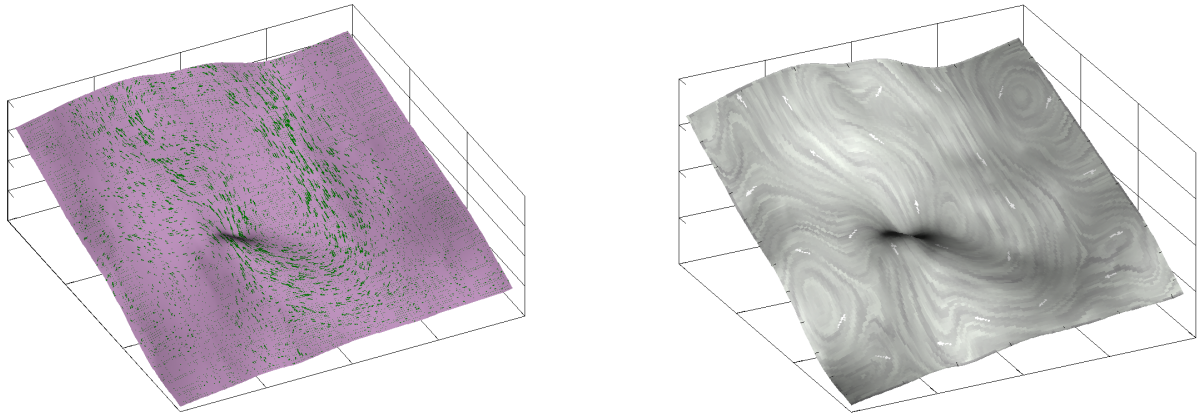


Fig. 7. Overlaying  $\mathbf{w}$  helps highlight locations of strongly beating nanorods in the image. Overlay is presented both as quiver (left) and LIC (right).

We must now choose the acceleration,  $g$ , due to metaphorical gravity. Clearly, it must be at least great enough to match the largest force exerted by  $\mathbf{F}$ , so  $g \geq |\mathbf{F}|_{\max}$ , where  $|\mathbf{F}|_{\max}$  is the largest magnitude of  $\mathbf{F}$  over the area of the image. Aside from this constraint, we are apparently free to choose  $g$  as we please.

As explained in Section 2.1, we prefer the limiting case where  $\mathbf{m} = \mathbf{F}$ ; this is the case of  $g \gg |\mathbf{F}|_{\max}$ . To our knowledge, there is no reason to stray from this choice, though we note that choosing  $g = |\mathbf{F}|_{\max}$  suppresses discontinuities in  $\hat{\mathbf{m}}$  where they exist in  $\hat{\mathbf{F}}$ .

#### ACKNOWLEDGEMENTS

The authors wish to thank Art Champagne for helpful conversations regarding vector field decomposition, Brian Eastwood for the use of ImageTracker, and Adam Shields for his datasets of microfluidic transport. LIC was generated using Matlab code made available by Nima Bigdely Shamlo, available at [www.mathworks.com/matlabcentral](http://www.mathworks.com/matlabcentral). This work was supported by National Institute of Biomedical Imaging and Biotechnology grant P41-EB002025.

#### REFERENCES

- [1] A. Bruhn, J. Weickert, and C. Schnörr. Lucas/Kanade Meets Horn/Schunck: Combining Local and Global Optic Flow Methods. *International Journal of Computer Vision*, 61(3):211–231, 2005.
- [2] B. Cabral and L. Leedom. Imaging vector fields using line integral convolution. *Proceedings of the 20th annual conference on Computer graphics and interactive techniques*, pages 263–270, 1993.
- [3] J. Ebling and G. Scheuermann. Clifford Convolution And Pattern Matching On Vector Fields. *Proceedings of the 14th IEEE Visualization 2003 (VIS'03)*, 2003.
- [4] B. Evans, A. Shields, R. Carroll, S. Washburn, M. Falvo, and R. Superfine. Magnetically Actuated Nanorod Arrays as Biomimetic Cilia. *Nano Lett*, 7(5):1428–1434, 2007.
- [5] R. Frankot and R. Chellappa. A method for enforcing integrability in shape from shading algorithms. *IEEE Transactions on Pattern Analysis and Machine Intelligence*, 10(4):439–451, 1988.
- [6] R. Kirby, H. Marmanis, and D. Laidlaw. Using concepts from painting. *Visualization'99. Proceedings*, pages 333–540, 1999.
- [7] D. Laidlaw, R. Kirby, C. Jackson, J. Davidson, T. Miller, M. da Silva, W. Warren, and M. Tarr. Comparing 2D Vector Field Visualization Methods: A User Study. *IEEE Transactions on Visualization and Computer Graphics*, 11(1):59–70, 2005.
- [8] D. Laser and J. Santiago. A review of micropumps. *J. Micromech. Microeng*, 14(6):35–64, 2004.
- [9] W. Lefer, B. Jobard, and C. Leduc. High-Quality Animation of 2D Steady Vector Fields. *IEEE Transactions on Visualization and Computer Graphics*, 10(1):2–14, 2004.
- [10] N. Nguyen and Z. Wu. Micromixers review. *J. Micromech. Microeng*, 15(2):R1–R16, 2005.
- [11] K. Polthier and E. Preuss. *Variational Approach to Vector Field Decomposition*. SFB 288; Niedersächsische Staats-und Universitätsbibliothek, 2000.
- [12] K. Polthier and E. Preuss. Identifying Vector Fields Singularities using a Discrete Hodge Decomposition. *Visualization and Mathematics*, 3:113–134, 2003.
- [13] T. Preusser and M. Rumpf. Anisotropic nonlinear diffusion in flow visualization. *Visualization'99. Proceedings*, pages 325–539, 1999.
- [14] A. Sanderson, C. Johnson, and R. Kirby. Display of vector fields using a reaction-diffusion model. *Visualization, 2004. IEEE*, pages 115–122, 2004.
- [15] H. Shen and D. Kao. A new line integral convolution algorithm for visualizing time-varying flow fields. *IEEE Transactions on Visualization and Computer Graphics*, 4(2):98–108, 1998.
- [16] A. Telea and J. van Wijk. Simplified representation of vector fields. *Proceedings of the conference on Visualization'99: celebrating ten years*, pages 35–42, 1999.
- [17] Y. Tong, S. Lombeyda, A. Hirani, and M. Desbrun. Discrete multiscale vector field decomposition. *ACM Transactions on Graphics*, 22(3):445, 2003.
- [18] G. Turk and D. Banks. Image-guided streamline placement. *Proceedings of the 23rd annual conference on Computer graphics and interactive techniques*, pages 453–460, 1996.
- [19] T. Urness, V. Interrante, I. Marusic, E. Longmire, and B. Ganapathisubramani. Effectively visualizing multi-valued flow data using color and texture. *IEEE Visualization*, pages 115–122, 2003.
- [20] J. van Wijk. Spot noise texture synthesis for data visualization. *ACM SIGGRAPH Computer Graphics*, 25(4):309–318, 1991.
- [21] V. Verma, D. Kao, and A. Pang. PLIC: bridging the gap between streamlines and LIC. *Proceedings of the conference on Visualization'99: celebrating ten years*, pages 341–348, 1999.
- [22] C. Ware and W. Knight. Using visual texture for information display. *ACM Transactions on Graphics (TOG)*, 14(1):3–20, 1995.
- [23] D. Weiskopf, G. Erlebacher, and T. Ertl. A Texture-Based Framework for Spacetime-Coherent Visualization of Time-Dependent Vector Fields. *Proceedings of the 14th IEEE Visualization 2003 (VIS'03)*, 2003.